Science and Technology Indonesia
e-ISSN:2580-4391 *p*-ISSN:2580-4405
Vol. 9, No. 3, July 2024

Research Paper

Application of $KBaYSi_2O_7:Bi^{3+},Eu^{3+}$ Phosphor for White Light-Emitting Diodes with Excellent Color Quality

Nguyen Thi Phuong Loan[1], Le Xuan Thuy[2], Nguyen Le Thai[3], Hsiao Yi Lee[4], Pham Hong Cong[5]*

[1]*Faculty of Fundamental 2, Posts and Telecommunications Institute of Technology, Ho Chi Minh City, 710547, Vietnam*
[2]*Faculty of Basic Sciences, Vinh Long University of Technology Education, Vinh Long Province, 890000, Vietnam*
[3]*Faculty of Engineering and Technology, Nguyen Tat Thanh University, Ho Chi Minh City, 754000, Vietnam*
[4]*Department of Electrical Engineering, National Kaohsiung University of Science and Technology, Kaohsiung City, 824005, Taiwan*
[5]*Faculty of Electrical Engineering Technology, Industrial University of Ho Chi Minh City, Ho Chi Minh City, 727900, Vietnam*
***Corresponding author**: phamhongcong@iuh.edu.vn

Abstract
This paper examines the properties of two phosphor materials synthesized via utilizing the sol gel method: $KBaYSi_2O_7:Bi^{3+}$ (KBYS:Bi) phosphor providing cyan/deep-blue emission and $KBaYSi_2O_7:Bi^{3+},Eu^{3+}$ (KBYS:Bi,Eu) phosphor exhibiting tunable emission from near-UV to red. The optimal doping concentrations for Bi^{3+} and Eu^{3+} are 0.2% and 3.5%, respectively. It is found that the ability to give discrepant emission peaks under different excitation sources of the KBYS:Bi phosphor is attributed to the occupancy of Bi^{3+} in different cation hosts. Meanwhile, co-doping the Eu^{3+} and Bi^{3+} into the KBYS host leads to red and cyan emission regions, enabling the emission tunability of the KBYS:Bi,Eu phosphor. KBYS:Bi,Eu phosphor was then used in combination with $YAG:Ce^{3+}$ and blue chips to fabricate a white light emitting diode (LED) model. The particle sizes of KBYS:Bi,Eu phosphor are adjusted to examine its influences on the LED properties. With increasing particle sizes (≥12 μm), the KBYS:Bi,Eu phosphor can improve the scatter efficacy, transmission power, lumen output, and color performance (rendition and uniformity). Both KBYS:Bi and KBYS:Bi,Eu phosphors are promising luminescent phosphors that can be combined with other phosphor with different emission colors to obtain the full-spectrum or tunable white light for LEDs.

Keywords
$KBaYSi_2O_7:Bi^{3+}$, $YAG:Ce^{3+}$, LEDs, Lumen Output, Color Quality

Received: 9 February 2024, Accepted: 25 April 2024
https://doi.org/10.26554/sti.2024.9.3.756-765

1. INTRODUCTION

The solid-state lighting technology featuring white-illuminating diodes (WLEDs) in the form of illumination means has become essential for advanced optical applications (Asano et al., 2013; Boisier et al., 2009; Chang et al., 2013). Compared to other sources of illumination, such as incandescent bulbs, LEDs offer more significant utilization benefits, including environmental friendliness, long-term service, and energy efficiency. Therefore, LEDs have been applied in many aspects, not only in regular household lighting but also in displaying, transporting, and medical trackers (Chen et al., 2013; Cheng et al., 2016; Chou et al., 2012). Commonly, there are two ways to produce white light for LED, including the combination of multiple phosphors with different emission colors and the integration of tri-color chip set. Notably, LEDs fabricated by combining phosphor materials with LED chips are more favorable than those created with tri-color chip set. The former is simpler to design and modify to obtain desirable white light performances. The most common luminescent phosphor in use is YAG:Ce with yellow luminescence. It was recorded that the luminosity of the LED comprising YAG:Ce and blue chip was high. However, the phosphor concentration used for the phosphor sheet on the chips was significant, resulting in a high temperature in the package. Moreover, the color rendering efficiency of this LED type is poor for advanced devices requiring high visual reproduction. This drawback results from the insufficient red-light energy in the generated light. To address this problem, the red-phosphor materials were introduced to the multi-phosphor packaging method to improve the red-spectrum energy (Costa et al., 2020; Pardo et al., 2012; Frank et al., 2020). In particular, the combination of blue, red, and green phosphors has been applied to achieve the full spectrum white light for ultraviolet (UV)/near-UV LEDs. Nevertheless, the broad cyan spectral band gap of 480 nm – 520 nm caused the reduction of color clarity and rendition, making it hard to accomplish a

full-spectrum white light. The cyan-emission phosphors were developed and proposed to bridge such a spectral gap. The Eu^{2+} and Ce^{3+} are popular ion dopants for being incorporated into organic phosphor hosts to produce such phosphors. Regardless, the absorption spectra for those cyan-luminescent phosphors fail to match UV and/or near-UV LED chips (Frank et al., 2019; Ho, 1999). Moreover, another critical issue with phosphors featuring Eu^{2+} and Ce^{3+} as activators is the unavoidable light absorption in the visible range, which hinders the lumen efficiency of the white LED device (Jin et al., 2018; López Esmerio et al., 2022; Kadhem, 2023).

The non-rare earth ion Bi^{3+} can become an efficient alternative to the divalent Eu and trivalent Ce for possessing outstanding spectral characteristics. Specifically, the lanthanide ion Bi^{3+} can show a broadband emission from cyan to red regions and absorption bands, depending on the selected hosts. Additionally, its absorption band is almost in the near-UV with no emission overlap in the visible light region, effectively limiting the visible-light reabsorption. Besides, the naked orbit 6s-6p of the Bi^{3+} enables its tunable emission by adjusting the host lattice environment (Li et al., 2019; Yan et al., 2019; Xie et al., 2019). Several cyan phosphors with Bi^{3+} as activators were introduced, such as $LiGd_5P_2O_{13}$:Bi^{3+} (Wang et al., 2017), Sr_2LaGaO_5:Bi^{3+} (Liu et al., 2019a), and (Ba,Sr)$3Sc_4O_9$:Bi^{3+} (Dang et al., 2018). However, these cyan phosphors still show spectral issues including the high incompatibility with the near-UV chip excitation, high thermal quenching, and low quantum efficiency. Hence, the search for effective Bi^{3+}-doped cyan phosphor is ongoing.

As the orange-red emission is important to the color rendering performance of the white LED, effective red-emitting phosphors prove to be an appealing subject for researchers. One of the popular red-emission activators is the trivalent europium (Eu^{3+}). Several reports demonstrate that Eu^{3+}-doped phosphors show great photoluminescence with their emission peaks located in the red regions (603-650 nm) owing to the energy transition of ion 5D0–7F2 (Arantes et al., 2019; Zhao et al., 2021). However, most commercial phosphor yield low efficacy, chemical instability, and poor near-UV excitability (Khachatourian et al., 2016; Limbu et al., 2020). As such, to improve the efficiency of Eu^{3+}, appropriate sensitizers are introduced into the same host. In this manner, the obtained phosphor can generate tunable emissions and/or improved red emissions, depending on the ion co-doped with the Eu^{3+}. For instance, a stronger red emission of Eu^{3+} was obtained by co-doping with Sm^{3+} (Wu et al., 2019; Lephoto et al., 2018). Tunable emission of green-to-red range was achieved with the ion pairs of Eu^{3+}/Tb^{3+} (Ahemen and Dejene, 2017) while red-to-deep red emission for high-sensitive luminescent thermometry was obtained by pairing Eu^{3+} with Mn^{4+} (Shi et al., 2023; Tang et al., 2022).

To the best of our knowledge, reports on phosphors with tunable emissions from cyan to red are rare. In addition, the ion Bi^{3+} is a good sensitizer for other lanthanide ions to enhance their emission strengths (Hsu and Cheng, 2021; Jiang et al., 2013). Thus, when co-doping Bi^{3+} with another lanthanide ion, it is possible to achieve tunability for the phosphor luminescence. As a result, combining Eu^{3+} and Bi^{3+} can be a solution to augment red luminescence while introducing the cyan-emission bridge to the generated white-light spectrum. On the other hand, emission-tunable phosphors have earned substantial recognition in modern solid-state illumination technology owing to their multi-functionality and lesser complexity in fabrication, compared to conventional multi-phosphor packages. This paper discusses the preparation for the $KBaYSi_2O_7$:Bi^{3+} (KBYS:Bi) and $KBaYSi_2O_7$:Bi^{3+},Eu^{3+} (KBYS:Bi,Eu) phosphors. The $KBaYSi_2O_7$ (KBYSO) phosphor is an appropriate host for doping activators ions like the Bi^{3+} and Eu^{3+} owing to its monoclinic crystalline configuration, enabling better stability in thermal, chemical, and structural properties of the prepared phosphors. When doping Bi^{3+} and Eu^{3+} ions, to ensure their occupancy in the host cations, it is essential that the difference percentage between their and cations' radii must be less than 30%. This parameter, radius difference (Rd), can be estimated using Equation (1) (Li et al., 2018):

$$Rd = 100 \times \frac{[R_h(CN) - R_d(CN)]}{[R_h(CN)]} \quad (1)$$

R_h(CN) and R_d(CN) represent the radii for the base cation and the incorporating ion, respectively. CN is the abbreviation of the coordination number. The cations in the KBYSO host include K^+, Y^{3+}, and Ba^{2+} for which the Eu^{3+} and Bi^{3+} can be utilized as substitutes. The estimated Rd between the Eu^{3+} ion and K^+ and Ba^{2+} was significantly larger than 30%, while that between Eu^{3+} and Y^+ was much smaller than 30%. This indicates that the occupancy of Eu^{3+} takes place in the Y^+ cation. On the other hand, in the Bi^{3+} case, the R_d between its radius and these three cations was less than 30%. However, the R_d with K^+ is the largest, indicating that the substitution of Bi^{3+} was more likely to occur in the Y^+ and Ba^{2+} host cations. Additionally, with the use of Kubelka Munk function (Kumar et al., 2017), it is possible to verify the optical band gap of the KBYS phosphor. The obtained result was particularly high, >4.0 eV based on the absorption spectra, indicating that the synthesized phosphors could generate a high luminescence by containing the Eu^{3+} or Bi^{3+} energy levels.

In this work, the KBYS:Bi with cyan emission can contribute to bridging the cyan spectral gap while the KBYS:Bi,Eu may offer the tunable white-light emission for the white LED. The luminescence and thermostability of the phosphors will also be assessed. Afterwards, the KBYS:Bi,Eu is utilized to create a white LED model. The influences of this phosphor on the LED lighting performance are then discussed. The obtained results reveal that the KBYS:Bi,Eu phosphor can be appropriate for creating cold to warm white LED lights. The experimental section (section 3) will demonstrate the preparation of the KBYS:Bi,Eu phosphor and the examined white LED model. The computational discussion is included to investigate the characteristics of the phosphor and subsequently, the effects

of KBYS:Bi,Eu with varying particle diameters are presented, all of which are included in section 4. The final section is the conclusion of the paper, summarizing the obtained results and suggesting future works on the KBYS:Bi,Eu phosphor.

2. EXPERIMENTAL SECTION

2.1 Materials

The synthesizing method of KBYS:Bi and KBYS:Bi,Eu phosphors is the sol-gel approach (Jin et al., 2009; Kang et al., 2013; Kim et al., 2016). The chemical components essential for the phosphor synthesis are detailed in Table 1. Specifically, the raw materials include $Ba(NO_3)_2$ (reagent, 99%), $Eu(NO_3)_3$ (99.9%), and $Bi(NO_3)_3$ (reagent, 98%), all of which were obtained from Sigma-Aldrich (Wardhani et al., 2023; Novianty et al., 2023). The doping concentrations of Bi^{3+} for the KBYS:Bi compound were varied in the range of 0.08 – 0.8% and for the KBYS:Bi,Eu, the concentration was 0.2%. Meanwhile, the Eu^{3+} doping dosage ranged from 0.5% to 5.5%.

Table 1. Chemical Components for KBYS:Bi/KBYS:Bi,Eu Synthesis

Components	Amounts
$Ba(NO_3)_2$	2 mmol
$Bi(NO_3)_3$	0.08 - 0.8%
$Eu(NO_3)_3$	0.5 - 5.5%
Citric acid	4 mmol
Polyethylene glycol (PEG)	1 g
Ethyl orthosilicate (TEOS)	892 μL

2.2 Measurement Instruments

The measurement of the phosphor's photoluminescence excitation, photoluminescence spectra and decay curves were performed with an FLS980 spectrofluorometer (Edinburgh) featuring an excitation source of 150 W Xe lamp. The temperature-dependent luminescence was collected with an FLSP-920 spectrometer (Edinburgh) featuring a temperature controller (900-1100 degrees Celsius). For simulating the effects of KBYS:Bi,Eu phosphors on white LED properties, Mie-theory-based simulation and MATLAB program were utilized.

2.3 Preparation Procedures

The synthesizing process of KBYS:Bi and KBYS:Bi,Eu phosphors can be demonstrated as follows:

1. $Ba(NO_3)_2$, $Bi(NO_3)_3$/$Eu(NO_3)_3$, and citric acid with the listed amounts were thoroughly stir-blended with a solution of 40 mL water and 20 mL ethanol.
2. The nitric acid was added to regulate the pH level of the mixture to be between 3 – 4.
3. The PEG and TEOS with listed amounts were then added to the solution to form a transparent sol gel after stirring for 4 hours.
4. The gel was dried at 75 degrees Celsius in a water bath.
5. Then, this gel underwent a 3-hour preheating stage at 500 degrees Celsius.
6. Subsequently, the obtained sample was ground into powder, followed by a process of calcination at 900 – 1000 degrees Celsius for 1 – 5 hours.

The prepared KBYS:Bi,Eu phosphor was utilized for fabricating white LED models. It was combined with the yellow YAG:Ce^{3+} phosphor and near-UV LED chips (365 nm or 310 nm). The model of white LED used in this work is introduced in Figure 1. Particularly, Figure 1(a) depicts the actual LED apparatus, Figure 1(b) shows LED chips' wire bonding, Figure 1(c) illustrates the internal arrangement of LED components, and Figure 1(d) exhibits the LED simulation as a 3D formation created via the LightTools software (Kumar et al., 2017; Lee et al., 2010; Li et al., 2020).

3. RESULTS AND DISCUSSION

3.1 Luminescent Performance of the KBYS:Bi,Eu Phosphors

The transference between the Eu^{3+} and Bi^{3+} energy levels can be computed with the critical distance (D_c) (Lissner and Urban, 2011), which is expressed in Equation (2). On the other hand, the multipole electron interactions are often responsible for the energy transfer of trivalent rare-earth ions, which can be defined using the expression in Equation (3):

$$D_c = 2 \times \left[\frac{3V}{4\pi X_C Z}\right]^{\frac{1}{3}} \quad (2)$$

$$I_e/x = \frac{k}{\left[1 + \beta\,(x)^{\theta/3}\right]} \quad (3)$$

In Equation (2), V, X_c, and Z indicate the unit-cell volume, the critical dopant dosage, and the host's coordination number, respectively. In Equation (3), I_e is the intensity of emission, resulting in I_e/x demonstrating the emission strength at a specific concentration value. Additionally, k and β are constants. For the KBYS:Bi phosphor, the optimal concentration of Bi^{3+} was fixed at 0.2% as this number gave the highest recorded luminescence values for the KBYS:Bi sample. The KBYS:Bi phosphor could emit different luminescence colors under different excitation wavelengths. Specifically, while the broad emission band ranges from 350 nm to 650 nm when recording the luminescence of KBYS:Bi phosphor under 328 nm and 365 nm excitations, the first induced an emission peak in the cyan region (489 nm), while the latter generated a peak in the deep blue region (412 nm). This could be ascribed to the replacement of the Bi^{3+} with the electronic transition of 1S0→3P1 at the Ba^{2+} (cyan) and Y^{+} (deep blue) cation sites. The temperature-dependent luminescent intensities of the KBYS:Bi phosphor were also recorded with varying temperature values (900-1100 degrees Celsius). The highest intensity was observed with the temperature of 1000 degrees Celsius, while increasing the temperature to 1100 degrees Celsius reduced the sample's luminescence. The reduction of KBYS:Bi

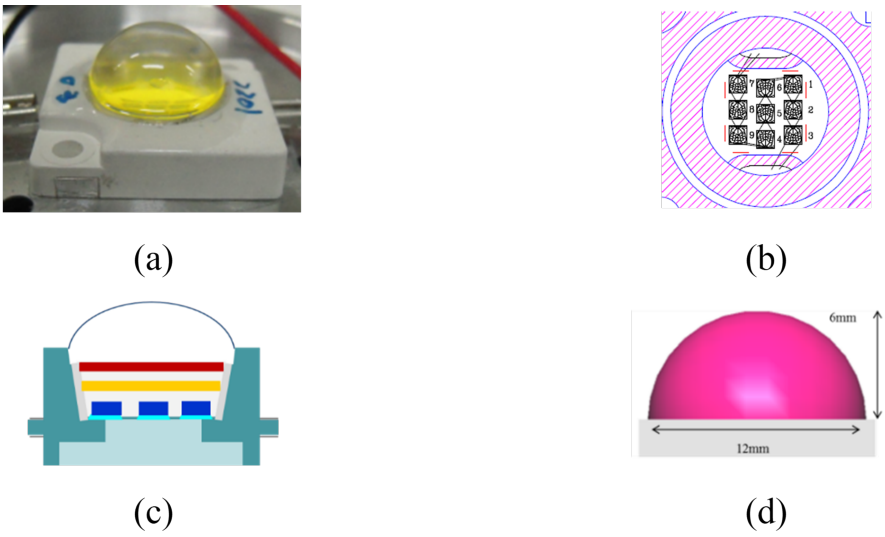

Figure 1. The LED Model Illustration: (a) an Actual White LED, (b) LED-Chips' Wire Bonding, (c) Components Arrangement, (d) White-LED Simulation Created with LightTools Software

luminescence at a higher annealing temperature could be attributed to the temperature quenching induced by the initiated impurity phase in the host environment.

Next, the luminescence of the KBYS:Bi,Eu phosphor was examined. When monitoring with the emission spectra of 489 nm or 610 nm, the highest excitation spectrum was perceived at 328 nm, which is probably induced by the electric transition of the Bi^{3+}. This implies that both Eu^{3+} and Bi^{3+} activators could be excited with the 328 nm band. When observing the luminescence of the KBYS:Bi,Eu phosphor under the 328 nm excitation band, a wide band centered at 489 nm for Bi^{3+} and sharp peaks for Eu3+, being most noticeable at 610 nm, could be recorded. As such, it could be expected that co-doping Bi^{3+} and Eu^{3+} could induce tunable emission spectra for the KBYS phosphor. The optimal concentration of Eu^{3+} dopants in this phosphor compound was found to be 3.5%. With enhancing doping concentration of Eu^{3+}, the emission intensity of Eu^{3+} was improved while that of Bi^{3+} was gradually decreased, owing to the energy transfer process between the Eu^{3+} and Bi^{3+}. This can be also proven with the measurement of luminescence decay lifetimes of KBYS:Bi,Eu, which was fitted with the double exponential function (Liu et al., 2019b; Li et al., 2020, as shown in Equations (4) and (5):

$$I_T = A_1 \exp(-T/\tau_1) + A_2 \exp(-T/\tau_2) \quad (4)$$

$$\tau = (A_1\tau_1^2 + A_2\tau_2^2)/(A_1\tau_1 + A_2\tau_2) \quad (5)$$

where T denotes the time, resulting in I_T representing the intensity of luminescence at T. A_1 and A_2 represent constant values, while τ_1 and τ_2 represent lifetimes of the phosphor compound. Since the increasing concentration of Eu^{3+} resulted in the decreasing Bi^{3+} luminescent lifetime, the presence of Bi^{3+} to Eu^{3+} energy transfer was proven. These results indicate that both KBYS:Bi and KBYS:Bi,Eu phosphors are promising luminescent phosphor compounds for fabricating white LEDs. The KBYS:Bi phosphor offering cyan to deep-blue emissions can be combined with other phosphors of blue, yellow-green, and red luminescence to acquire a full-spectrum white light for LEDs. Meanwhile, with the KBYS:Bi,Eu phosphor, it is possible to obtain cold to warm white light by adjusting the Eu^{3+} doping dosage in the host.

3.2 Effects of KBYS:Bi,Eu on White-LED Properties

The KBYS:Bi,Eu phosphor, when added into the phosphor layer of the white LED package, had noticeable impacts on the scattering performance of the package, as can be seen in Figure 2. The scattering coefficient (SC) of the LED light was monitored with different particle sizes of KBYS:Bi,Eu phosphor from 2 to 8 μm, see Figure 2(a) – (k). In general, adding and increasing the particle sizes of KBYS:Bi,Eu phosphor induced the SCs. Specifically, smaller particle sizes ($\leq$12 μm) benefitted the SC values for near-UV and short blue emission wavelengths, while larger particle sizes (14-20 μm) stimulated the scattering of longer wavelengths located in the green-to-red regions. This means that smaller phosphor particles induced the LED chips' light, while larger particles helped induce the conversion efficiency of longer-wavelength lights, including the orange-red ones, for the improvement of color rendition of the LED.

With the KBYS:Bi,Eu phosphor combined with the YAG:Ce^{3+} phosphor to build the white LED models in this work, changes in the KBYS:Bi,Eu particle sizes could affect the doping concentration of the YAG:Ce^{3+} yellow phosphor. This influence is displayed in Figure 3, in which the concentration of YAG:Ce^{3+} declines under the increasing radius of the

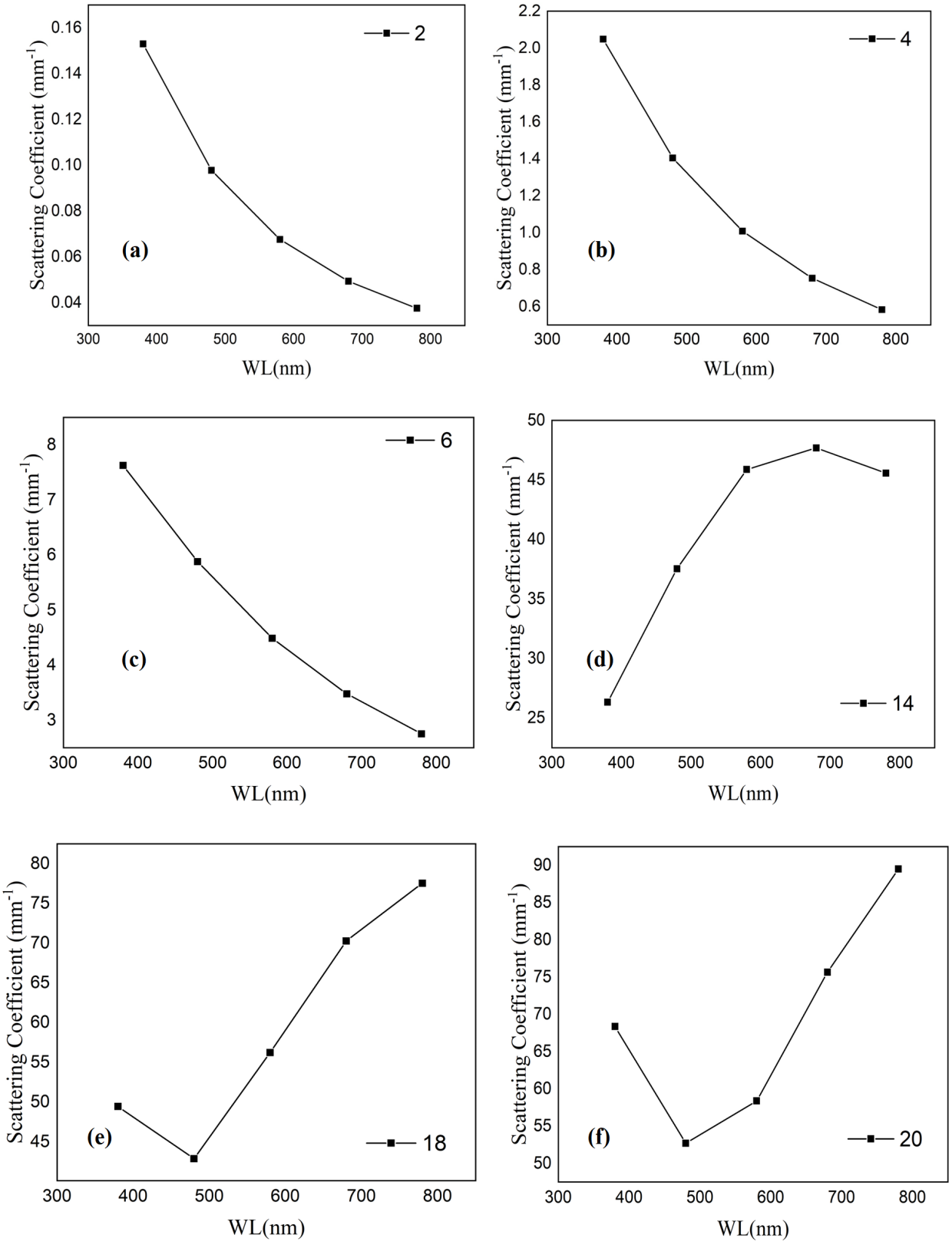

Figure 2. Scattering Coefficients of KBYS:Bi,Eu Phosphor Particles at: (a) 2 μm; (b) 4 μm; (c) 6 μm; (d) 14 μm; (e) 18 μm; (f) 20 μm

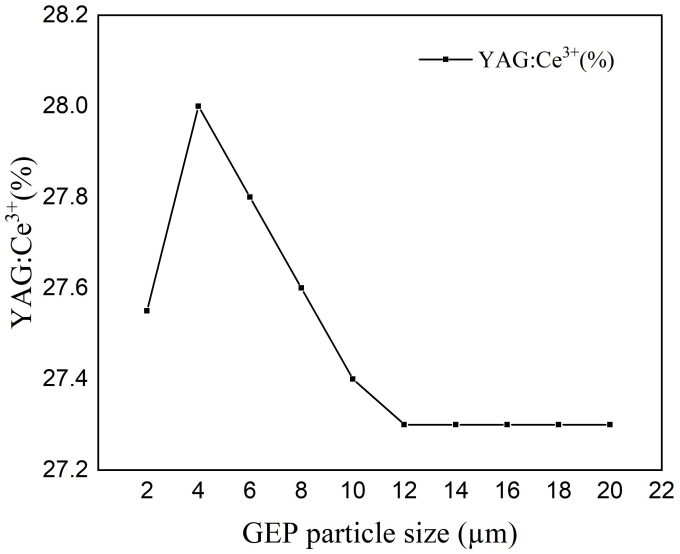

Figure 3. Changes in YAG:Ce^{3+} with Different KBYS:Bi,Eu Particle Sizes

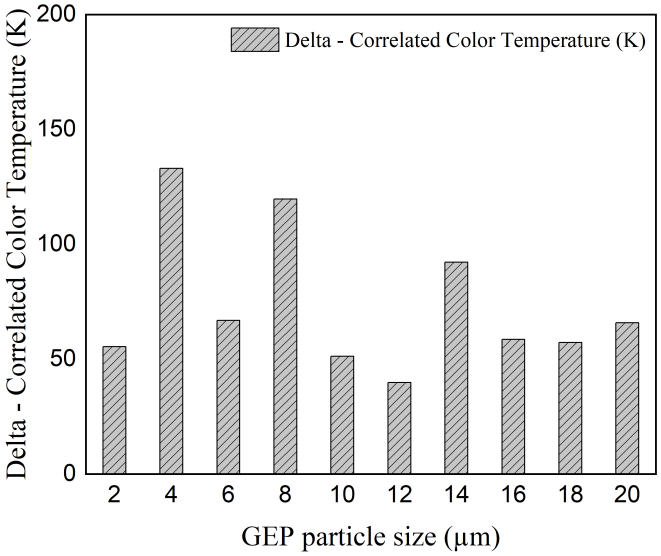

Figure 5. The CCT Differences with Different KBYS:Bi,Eu Particle Sizes

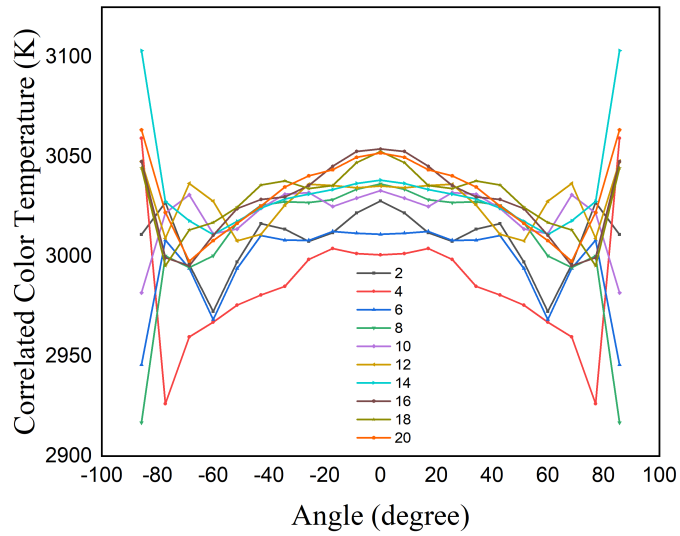

Figure 4. Changes in CCT Values of the LED Light with Different KBYS:Bi,Eu Particle Sizes

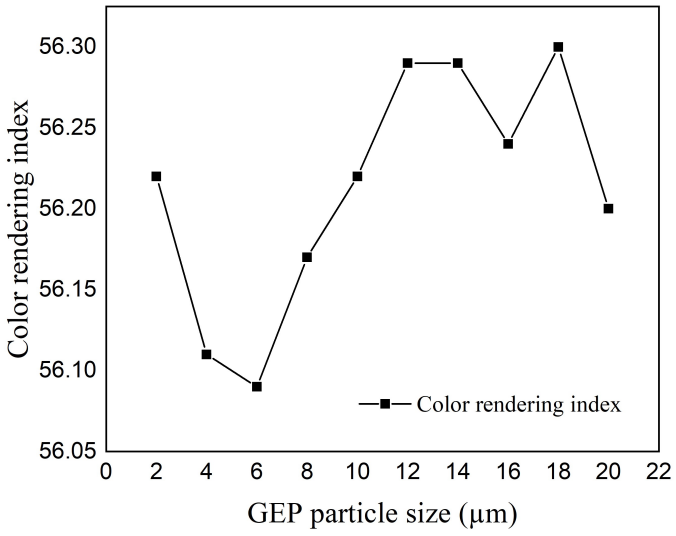

Figure 6. CRI Values with Different KBYS:Bi,Eu Particle Sizes

KBYS:Bi,Eu particles. It can be noticed that the YAG:Ce^{3+} surged with the small KBYS:Bi,Eu particle size of 4 µm then gradually decreased with larger particles doped in the phosphor layer. When KBYS:Bi,Eu particle sizes reached 12-20 μm, the YAG:Ce^{3+} concentration was maintained at its lowest values. This could be ascribed to the scattering effects of the phosphor layer in the presence of KBYS:Bi,Eu. With the 4 μm property, the scattering of blue light was strong, making the correlated color temperature (CCT) more likely to be cold. As such, the YAG:Ce^{3+} would be high to provide more converted yellow lights to balance the CCT values. With a larger KBYS:Bi,Eu radius, the YAG:Ce^{3+} concentration decreased as the conversion of light with longer wavelengths was enhanced, and the CCT shifted to the warmer side. Apart from keeping the CCT stability, the change in YAG:Ce^{3+} helped regulate the luminescence and color rendering performance of the LED light as the KBYS:Bi,Eu particle sizes were modified (Liu et al., 2012; Takagi et al., 2011).

The changes in CCT with different KBYS:Bi,Eu particle radii are shown in Figure 4. Then, the difference in CCT values when increasing the KBYS:Bi,Eu granules' sizes in the layer is depicted in Figure 5. As can be seen, the addition KBYS:Bi,Eu phosphor resulted in the warm white light with

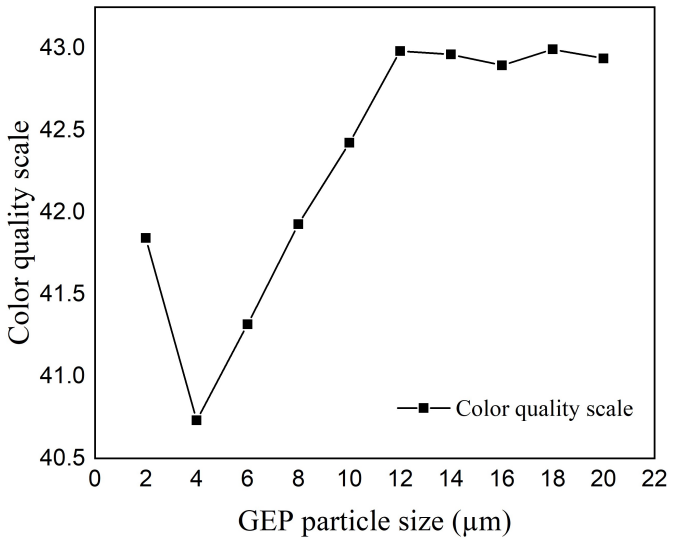

Figure 7. CQS Values with Different KBYS:Bi,Eu Particle Sizes

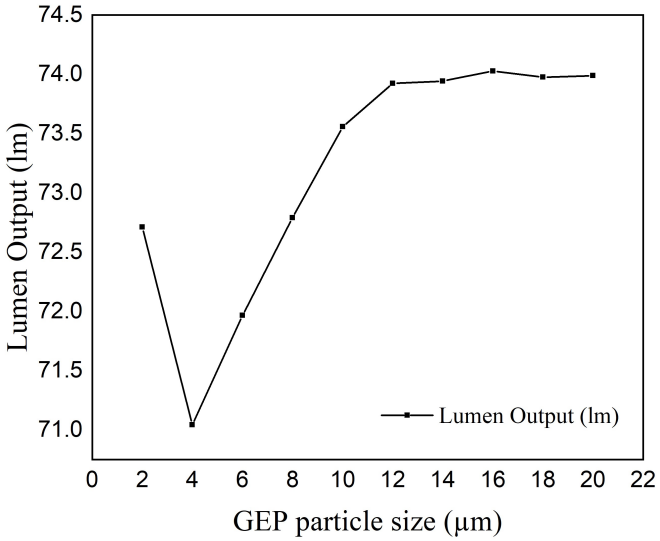

Figure 9. Lumen output of the LED light with different KBYS:Bi,Eu particle sizes

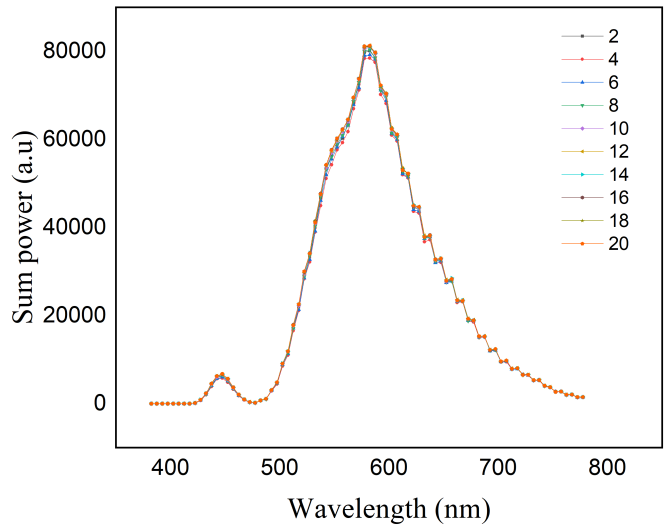

Figure 8. The Transmission Power of LED Light with Different KBYS:Bi,Eu Particle Sizes

the CCT around 3100 K. Overall, the surge in the phosphor sizes reduced the difference in CCTs. The highest CCT difference was acquired when the KBYS:Bi,Eu radius was at 4 μm, and the smallest value was recorded with 12 μm particles. The smaller CCT deviation denotes higher color stability and uniformity. Therefore, the KBYS:Bi,Eu phosphor can contribute to augmenting the color uniformity of the LED light (Tsai et al., 2011; Konovalenko et al., 2021).

In terms of the color rendition performance, color rendering intent (CRI), and color quality scale (CQS) were examined. Our results suggest that increasing the particle size of KBYS:Bi,Eu phosphor can improve the CRI as well as CQS parameters for white LED apparatuses, as illustrated in Figures 6 as well as 7, respectively. They both declined with the KBYS:Bi,Eu radius being roughly 4 μm. As mentioned, when the particle size of the phosphor reached 4 μm, the emission of blue light from LED chips was stimulated, while the longer-wavelength lights, including green and red, were weaker. As a result, the color rendering efficiency was degraded. The larger particle sizes of KBYS:Bi,Eu phosphor augmented the conversion of longer-wavelength lights, thus gradually boosting the CRI and CQS. This also indicates that the red-light spectrum was sufficiently added to the white-light spectrum. Besides, though the CRI line suffered from a fluctuation when the phosphor particle sizes were more than 12 μm and started to decrease again when the phosphor radius was >18 μm, the CQS was more stable and the increase was more noticeable. As the CQS includes the CRI in its assessing factors, apart from the color coordination and viewer's inclination, the CQS is more precise and difficult to manage (Li et al., 2013). Therefore, with the notable improvement in CQS, and CRI, the KBYS:Bi,Eu proved itself to be a potential candidate for the higher color performance of white LED light.

The addition of KBYS:Bi,Eu phosphor with increasing particle radii also enhanced the light transmission efficiency and lumen output of the LED light. The transmission of light was induced in the presence of the KBYS:Bi,Eu as demonstrated by Figure 8. The peaks at 450 nm (blue) and ~595 nm (orange) were recorded. Moreover, the intensity at the 595 nm region was much sharper than the other, indicating that the orange-red emission was efficiently supplemented. The lumen output of the LED light in Figure 9 showed a similar trend to that of the CQS. The lowest lumen was noted with 4 μm KBYS:Bi,Eu particles while the larger particles stimulated the lumen strength. The highest lumen was seen with the particle size of KBYS:Bi,Eu phosphor of around 16 μm. This

was because the larger particles allowed additional light to pass through and escape from the LED encapsulation. In other words, the larger particles encouraged the extraction efficacy of light in the LED, leading to the improvement of the package's lumen. Subse3quently, the KBYS:Bi,Eu can be used with large particle sizes of 12-20 μm to achieve significant enhancements of the lumen and color rendition performances.

4. CONCLUSIONS

This work demonstrates the KBYS:Bi with cyan/deep-blue emission and KBYS:Bi,Eu with tunable emission from near-UV to red synthesized via the sol gel method. The optimal concentrations of Bi^{3+} and Eu^{3+} dopants were 0.2% and 3.5%, respectively. The KBYS:Bi phosphor showed cyan emission (489 nm) under an excitation of 328 nm and deep blue emission (412 nm) under a 365 nm excitation, due to the substitution of Bi^{3+} in different cations of the KBYS host. The KBYS:Bi,Eu phosphor, on the other hand, showed sharp emissions of 489 nm and 610 nm. It is possible to tune the color emission of white light from cold to warm by varying the Eu^{3+} doping concentration. When combined with YAG:Ce^{3+} and blue LED chips, the larger sizes of KBYS:Bi,Eu phosphor could improve the conversion efficiency and scattering productivity of both short and long-wavelength lights. The increasing radii of KBYS:Bi,Eu particle also supported the chroma consistency and manifesting performance of the LED light. Thus, the tunable-emission KBYS:Bi,Eu phosphor has a high probability of producing high-quality LED packages with improved optical properties.

5. ACKNOWLEDGMENT

We would like to express our gratitude to Prof. Hsin-Yi Ma, Department of Industrial Engineering and Management, Minghsin University of Science and Technology, for helping to establish this research.

REFERENCES

Ahemen, I. and F. Dejene (2017). Luminescence and Energy Transfer Mechanism in Eu^{3+}/Tb^{3+}-Co-Doped ZrO_2 Nanocrystal Rods. *Journal of Nanoparticle Research*, **19**(1); 1–15

Arantes, D. C., C. de Mayrinck, J. D. Santos, L. F. Maia, L. F. Oliveira, M. A. Schiavon, D. Pasquini, R. C. de Lima, L. C. de Morais, and J. Esbenshade (2019). Effect of Structural and Eu^{3+} Amount in TiO_2 Semiconductor Material on Down-conversion Photoluminescence Properties. *Optical Materials*, **88**(February); 522–533

Asano, T., T. Kondo, and S. Maeda (2013). Unified Evaluation Method of White Uniformity for Electronic Displays. In *IECON 2013-39th Annual Conference of the IEEE Industrial Electronics Society*. IEEE, pages 8341–8345

Boisier, B., A. Mansouri, P. Gouton, and P. Trollat (2009). Wine Color Characterization and Classification for Nuances Reproduction. In *2009 Fifth International Conference on Signal Image Technology and Internet Based Systems*. IEEE, pages 93–98

Chang, Y. Y., Z. Y. Ting, C. Y. Chen, T. H. Yang, and C. C. Sun (2013). Design of Optical Module with High Stability, High Angular Color Uniformity, and Adjustable Light Distribution for Standard Lamps. *Journal of Display Technology*, **10**(3); 223–227

Chen, K. J., H. V. Han, B. C. Lin, H. C. Chen, M. H. Shih, S. H. Chien, K. Y. Wang, H. H. Tsai, P. Yu, and P. T. Lee (2013). Improving the Angular Color Uniformity of Hybrid Phosphor Structures in White Light-Emitting Diodes. *IEEE electron device letters*, **34**(10); 1280–1282

Cheng, T., X. Yu, Y. Ma, B. Xie, Q. Chen, R. Hu, and X. Luo (2016). Angular Color Uniformity Enhancement of White LEDs by Lens Wetting Phosphor Coating. *IEEE Photonics Technology Letters*, **28**(14); 1589–1592

Chou, C. T., C. L. Lee, and T. L. Lin (2012). Color Temperature Compensation for LED Lighting Illumination. In *2012 International Conference on Machine Learning and Cybernetics*, volume 5. IEEE, pages 1784–1789

Costa, T., V. Gaudet, E. R. Vrscay, and Z. Wang (2020). Perceptual Colour Difference Uniformity in High Dynamic Range and Wide Colour Gamut. In *2020 IEEE International Conference on Image Processing (ICIP)*. IEEE, pages 161–165

Dang, P., S. Liang, G. Li, H. Lian, M. Shang, and J. Lin (2018). Broad Color Tuning of Bi^{3+}/Eu^{3+}-Doped (Ba, Sr) $3Sc_4O_9$ Solid Solution Compounds Via Crystal Field Modulation and Energy Transfer. *Journal of Materials Chemistry C*, **6**(37); 9990–9999

Frank, T., O. Haik, A. Jumabayeva, J. P. Allebach, and Y. Yitzhaky (2019). New Design for Compact Color Screen Sets for High-End Digital Color Press. *IEEE Transactions on Image Processing*, **29**(November); 3023–3038

Frank, T., O. Haik, A. Jumabayeva, J. P. Allebach, and Y. Yitzhaky (2020). New Design For Color Screen Sets For High-End Digital Color Press. In *2020 IEEE International Conference on Image Processing (ICIP)*. IEEE, pages 2566–2570

Ho, H. J. (1999). A New Approach Method to Improve the Brightness Uniformity in Color Display Tubes. In *ITE Technical Report 23.27*. The Institute of Image Information and Television Engineers, pages 75–78

Hsu, W.-Y. and H.-C. Cheng (2021). A Novel Automatic White Balance Method for Color Constancy under Different Color Temperatures. *IEEE Access*, **9**(August); 111925–111937

Jiang, M., W. Liang, and X. Zhang (2013). Perception-Based Color Space for Image Segmentation Application. In *2013 15th IEEE International Conference on Communication Technology*. IEEE, pages 625–628

Jin, H., P. Fengjuan, M. S. Molokeev, D. Junfeng, P. Mingying, Z. Weijie, and W. Jing (2018). Redefinition of Crystal Structure and Bi^{3+} Yellow Luminescence with Strong Nuv Excitation in La_3BWO_9:Bi^{3+} Phosphor for Wleds. *ACS Applied Materials & Interfaces (Print)*, **10**(16); 13660–13668

Jin, H., X. Zhao, and H. Liu (2009). Testing of the Uniformity of Color Appearance Space. In *2009 WRI World Congress on Computer Science and Information Engineering*, volume 6. IEEE, pages 307–311

Kadhem, S. J. (2023). Preparation of Al_2O_3/PVA Nanocomposite Thin Films by a Plasma Jet Method. *Science and Technology Indonesia*, **8**(3); 471–478

Kang, Y. R., K. H. Kim, W. H. Kim, S.-W. Jeon, M. S. Jang, J. S. Kwak, and J. P. Kim (2013). Utilization of Silicone Microspheres: Improving Color Uniformity and Reducing the Amount of Phosphor Used in White Light-Emitting Diodes. *IEEE Transactions on Components, Packaging and Manufacturing Technology*, **3**(9); 1453–1457

Khachatourian, A. M., F. Golestani-Fard, H. Sarpoolaky, C. Vogt, E. Vasileva, M. Mensi, S. Popov, and M. S. Toprak (2016). Microwave Synthesis of Y_2O_3: Eu^{3+} Nanophosphors: A Study on the Influence of Dopant Concentration and Calcination Temperature on Structural and Photoluminescence Properties. *Journal of Luminescence*, **169**(Part A); 1–8

Kim, J. E., J. W. Kim, and K. D. Kim (2016). Three-Dimensional Color Gamut for Color-Space-Modulation. In *2016 22nd Asia-Pacific Conference on Communications (APCC)*. IEEE, pages 409–413

Konovalenko, I. A., A. A. Smagina, D. P. Nikolaev, and P. P. Nikolaev (2021). ProLab: A Perceptually Uniform Projective Color Coordinate System. *IEEE Access*, **9**(September); 133023–133042

Kumar, H., S. Gupta, and K. Venkatesh (2017). Hole Correction in Estimated Depth Map from Single Image Using Color Uniformity Principle. In *2017 22nd International Conference on Digital Signal Processing (DSP)*. IEEE, pages 1–5

Lee, K. C., S. M. Kim, and J. H. Moon (2010). Improvement of Spatial Color Uniformity in White Light-Emitting Diodes with Self-Positioned Phosphor Layer. In *Asia Communications and Photonics Conference and Exhibition*. IEEE, pages 337–338

Lephoto, M. A., K. G. Tshabalala, S. J. Motloung, I. Ahemen, and O. M. Ntwaeaborwa (2018). Study on Photoluminescence and Energy Transfer of Eu^{3+}/Sm^{3+} Single-Doped and Co-Doped BaB_8O_{13} Phosphors. *Physica B: Condensed Matter*, **535**(April); 89–95

Li, C., B. Chen, D. Deng, H. Yu, H. Li, C. Shen, L. Wang, and S. Xu (2020). A Ratiometric Optical Thermometer with Tunable Sensitivity and Superior Signal Discriminability Based on Eu^{2+}/Eu^{3+} Co-Doped $La_1-yGdyAlO_3$ Phosphors. *Journal of Luminescence*, **221**(May); 117036

Li, H., X. Mao, Y. Han, and Y. Luo (2013). Wavelength Dependence of Colorimetric Properties of Lighting Sources Based on Multi-Color LEDs. *Optics Express*, **21**(3); 3775–3783

Li, H., R. Pang, Y. Luo, H. Wu, S. Zhang, L. Jiang, D. Li, C. Li, and H. Zhang (2019). Structural Micromodulation on Bi^{3+}-Doped $Ba_2Ga_2GeO_7$ Phosphor with Considerable Tunability of the Defect-Oriented Optical Properties. *ACS Applied Electronic Materials*, **1**(2); 229–237

Li, Z., Y. Tang, J. Li, C. Wu, X. Ding, and B. Yu (2018). High Color Uniformity of White Light-Emitting Diodes Using Chip-Scaled Package. *IEEE Photonics Technology Letters*, **30**(11); 989–992

Limbu, S., L. R. Singh, and G. S. Okram (2020). The Effect of Lithium on Structural and Luminescence Performance of Tunable Light-Emitting Nanophosphors for White LEDs. *RSC Advances*, **10**(59); 35619–35635

Lissner, I. and P. Urban (2011). Toward a Unified Color Space for Perception-Based Image Processing. *IEEE Transactions on Image Processing*, **21**(3); 1153–1168

Liu, D., P. Dang, X. Yun, G. Li, H. Lian, and J. Lin (2019a). Luminescence Color Tuning and Energy Transfer Properties in (Sr, Ba) $2LaGaO_5$:Bi^{3+}, Eu^{3+} Solid Solution Phosphors: Realization of Single-Phased White Emission for WLEDs. *Journal of Materials Chemistry C*, **7**(43); 13536–13547

Liu, S., Y. Liang, Y. Zhu, H. Li, J. Chen, and S. Wang (2019b). The Exploration of Structure Evolution and Photoluminescence Property in $Ca_9Al_{1-x}Y_x(PO_4)_7$:Eu^{2+} Solid Solution Phosphors Via the Construction of Bi-Directional Relationships. *Journal of Alloys and Compounds*, **785**(May); 573–583

Liu, Z. Y., C. Li, B. H. Yu, Y. H. Wang, and H. B. Niu (2012). Effects of YAG: Ce Phosphor Particle Size on Luminous Flux and Angular Color Uniformity of Phosphor-Converted White LEDs. *Journal of Display Technology*, **8**(6); 329–335

López Esmerio, C., C. Ruiz Rojas, J. Angulo Rocha, E. Lizárraga Medina, F. Ramos Brito, E. Camarillo García, R. Martinez Martinez, M. Aguilar Frutis, and M. García Hipólito (2022). Study of The Electrical, Optical and Morphological Properties in Submicron and Microstructured ZnO Thin Films Obtained by Spin Coating and Chemical Bath Deposition. *Science and Technology Indonesia*, **7**(3); 291–302

Novianty, E., S. Jorena, A. A. Bama, E. Koriyanti, M. Ariani, and I. Royani (2023). Synthesis of Fe(III)-IIPs (Ion Imprinted Polymers): Comparing Different Concentrations of HCl and HNO_3 Solutions in the Fe(III) Polymer Extraction Process for Obtaining the Largest Cavities in Fe(III)-IIPs. *Science and Technology Indonesia*, **8**(3); 361–366

Pardo, P. J., G. Martínez Borreguero, Á. L. Pérez, and M. I. Suero (2012). Worldwide Uniformity of Color Reproduction in Handheld Video-Game Consoles and Applications. *Journal of Display Technology*, **8**(4); 233–240

Shi, X., Y. Chen, G. Li, K. Qiang, Q. Mao, L. Pei, and J. Zhong (2023). Designing a Dual-Wavelength Excitation Eu^{3+}/Mn^{4+} Co-Doped Phosphors for High-Sensitivity Luminescence Thermometry. *Ceramics International*, **49**(12); 20839–20848

Takagi, Y., T. Asano, W. Liu, and J. Yao (2011). Color Uniformity Evaluation of Electronic Displays Based on Visual Sensitivity. In *2011 17th Korea-Japan Joint Workshop on Frontiers of Computer Vision (FCV)*. IEEE, pages 1–5

Tang, Q., N. Guo, Y. Xin, W. Li, B. Shao, and R. Ouyang (2022). Luminous Tuning in $Eu^{3+}Mn^{4+}$ Co-Doped Double Perovskite Structure by Designing the Site-Occupancy Strategy for Solid-State Lighting and Optical Temperature

Sensing. *Materials Research Bulletin*, **149**(May); 111704

Tsai, M. J., S. H. Chang, C. L. Lee, and C. T. Chou (2011). Color Quality Inspection and Compensation for Color LED-Display Modules. In *2011 International Conference on Machine Learning and Cybernetics*, volume 4. IEEE, pages 1720–1725

Wang, L., J. Qiao, Y. Liu, P. Huang, Q. Shi, Y. Tian, and Z. Luo (2017). Tunable Luminescence of The Full-Color-Emitting $LiGd_5P_2O_{13}$:Bi^{3+},Eu^{3+} Phosphor Based on Energy Transfers. *Optical Materials*, **67**(May); 78–83

Wardhani, S., H. A. Mardiansyah, and D. Purwonugroho (2023). Fe_3O_4-SiO_2-Alginate Photocatalyst for Textile Dyes Waste Degradation. *Science and Technology Indonesia*, **8**(1); 108–115

Wu, Y., K. Qiu, W. Zhang, and Q. Tang (2019). Synthesis and Luminescence Enhancement of Eu^{3+}/Sm^{3+} co-doped $Ca_9Bi(VO_4)_7$ Phosphor for White-Light-Emitting Diodes. *Journal of Materials Science. Materials in Electronics*, **30**(3); 3045–3054

Xie, T., L. Zhang, Y. Guo, X. Wang, and Y. Wang (2019). Tuning of Bi^{3+}-Related Excitation and Emission Positions through Crystal Field Modulation in the Perovskite-Structured $La_2(Zn_x, Mg_{1-x})TiO_6$ ($0 \leq x \leq 1$):Bi^{3+} Solid Solution for White LEDs. *Ceramics International*, **45**(3); 3502–3509

Yan, W., S. Chen, Y. Liu, Z. Gao, Y. Wei, and G. Li (2019). Giant Photoluminescence Improvement and Controllable Emission Adjustment in Bi^{3+}-Activated $Ca_4ZrGe_3O_{12}$ Phosphors for High-Quality White Light-Emitting diodes. *ACS Applied Electronic Materials*, **1**(9); 1970–1980

Zhao, J., H. Gao, H. Xu, Z. Zhao, H. Bu, X. Cao, and J. Sun (2021). Structure and Photoluminescence of Eu^{3+} Doped Sr_2InTaO_6 Red Phosphor with High Color Purity. *RSC Advances*, **11**(14); 8282–8289

